Separation Science and Technology
Publication details, including instructions for authors and subscription information:
http://www.informaworld.com/smpp/title~content=t713708471

Synthesis and Characterization of a Bentonite-Alginate Microspherical Adsorbent for Removal of Uranyl Ions from Aqueous Solutions

A. Tayyebi[a]; A. Khanchi[ab]; M. B. Ghofrani[a]; M. Outokesh[a]
[a] Department of Energy Engineering, Sharif University of Technology, Tehran, Iran [b] Jaber-ebne-Hayyan Laboratory, Nuclear Science and Technology Research Institute, Tehran, Iran

To cite this Article Tayyebi, A. , Khanchi, A. , Ghofrani, M. B. and Outokesh, M.(2010) 'Synthesis and Characterization of a Bentonite-Alginate Microspherical Adsorbent for Removal of Uranyl Ions from Aqueous Solutions', Separation Science and Technology, 45: 2, 288 — 298
To link to this Article: DOI: 10.1080/01496390903255903
URL: http://dx.doi.org/10.1080/01496390903255903

Separation Science and Technology, 45: 288–298, 2010
Copyright © Taylor & Francis Group, LLC
ISSN: 0149-6395 print/1520-5754 online
DOI: 10.1080/01496390903255903

Synthesis and Characterization of a Bentonite-Alginate Microspherical Adsorbent for Removal of Uranyl Ions from Aqueous Solutions

A. Tayyebi,[1] A. Khanchi,[1,2] M. B. Ghofrani,[1] and M. Outokesh[1]
[1]*Department of Energy Engineering, Sharif University of Technology, Tehran, Iran*
[2]*Jaber-ebne-Hayyan Laboratory, Nuclear Science and Technology Research Institute, Tehran, Iran*

A novel microspherical adsorbent for the removal of uranium from aqueous solutions was developed by immobilizing of natural bentonite in the polymeric matrix of calcium alginate. Different uptake properties of the prepared microspheres were examined using batch, stirred and column methods. The adsorbent showed high affinity toward uranium ions, especially at pHs above 3. Major uptake mechanisms included ion exchange, chelating of the $(UO_2)^{2+}$ ions to the $-OH$ groups of alginate, and surface complexation with bentonite. Surprisingly, the capacity of microspheres was higher than both its constituents, revealing that a synergetic effect occurs. Adsorption kinetics was controlled by slow chemical reaction of UO_2^{2+} ions with bentonite, and it obeyed a shrinking core model. Also a pseudo-second order chemical reaction fairly fitted the kinetics data. The synthesized microsphrese, in addition to cost efficiency, showed a relatively good column performance and high durability and reusability.

Keywords alginate microspheres; bentonite; reusability; selectivity; synergetic effect

INTRODUCTION

Bentonite clay, an abundant and inexpensive natural adsorbent seems to be very prominent for solving one of the greatest challenges of green chemistry “elimination and fixation of the radioactive elements from industrial effluents (1–5). Radioactive effluents arise primarily in uranium and thorium mining, during purification of uranium concentrate by solvent extraction, and most importantly in the reprocessing of the nuclear spent fuels (e.g., Purex process).

As for the treatment of the radioactive effluents, so far numerous methods have been developed including precipitation, solvent extraction, ion exchange, sorption on zeolite or other clay type adsorbents, adsorption by activated carbon, and more recently biosorption (6–11). Every method possesses some advantages and drawbacks. For instance, although solvent extraction has been successfully employed for removing of hazardous radio-cesium and strontium from high level liquid wastes at the Hanford reprocessing plant, it is nonetheless not technically appropriate for elimination of uranium from effluents of uranium extraction mills. This latter operation could be better done by ion exchange or adsorption processes (10).

Among the potential mineral adsorbents for treatment of industrial effluents, bentonite has one of the longest histories. From the early stage of developing ion exchange technology, an extensive study has been conducted on the characterization of bentonite that revealed its uptake properties for different radionuclide, as well as toxic heavy metals (2–4,12–14). Most of the undertaken research was carried out in the realm of the environmental concern about the migration of the hazardous ions in the soil that contains bentonite. Also, in a closely related study, some attempts were made on the application of bentonite as an artificial soil bed for the steel canisters which contain vitrified high level radioactive wastes. It was thought that bentonite, by adsorption, can deter the leaked ions of canisters from spreading in the environment and polluting underground waters.

Bentonite was also considered as a potential component of some adsorbents. The material for this purpose often has to be ground, washed, and chemically treated with mild acids or other appropriate solutions. But such treatments leave it with an inappropriate powdery form that is subject to considerable pressure loss in adsorption and carryover (by fluid) in backwash operations. Fortunately, the new fabrication techniques made it possible to modify the foregoing improper powdery form of the bentonite by its immobilization in a polymeric matrix (15). The result is a granular adsorbent quite similar to conventional ion exchange resins, which besides its better spherical shape encompasses greater attrition resistance and compression strength. The employed polymer for pelletizing of the bentonite must be a hydro gel to guarantee accessibility

---

Received 4 January 2009; accepted 15 July 2009.

Address correspondence to Mohammad Outokesh, Department of Energy Engineering, Sharif University of Technology, Azadi Ave. P.O. Box: 113658639, Tehran, Iran. E-mail: outokesh@sharif.ir or mohammad.outokesh@gmail.com

of the bentonite for water molecules and diffusing ions. So far, some synthetic polymers such as polyacrylamide and polyacrylontrile have been used for this service, but apparently there is no report about the application of biopolymer for the same purpose.

Biopolymers are selective, nontoxic, and cost efficient, and thus highly competitive with ion exchange resins. Among biopolymers, alginate is endowed with by its remarkable ion exchange properties, acid stability, and ease of sol-gel transformation (16–18). In fact, the water-soluble sodium alginate with high viscosity is able to disperse and stabilize both liquid droplets and solid particles, and the formed emulsion or suspension can be easily gelified and granulated through dripping in Ca^{2+} solutions (19–21). Calcium crosslink two adjacent alginate chains and thus gives rise to the formation of multinuclear microcapsules or microspheres (11).

In the current study, we attempted the synthesis of a bentonite-based adsorbent through its immobilization in the polymeric matrix of calcium alginate. The prepared microspherical adsorbent in addition to appreciable uptake properties is a biodegradable material and is able to concentrate uranium from aqueous solutions.

EXPERIMENTAL

Materials

Pulverized bentonite powder with an average particle size 40 μm was obtained from Esfahan mine (Iran), and used without further purification. Sodium alginate was purchased from BDH (England), and $UO_2(NO_3)_2$, $6H_2O$ and other reagents were supplied by Merck AG. (Germany).

Preparation of Microspheres

For simplicity, "NaALG" and "MSs" are used hereafter as abbreviations for "sodium alginate" and "microspheres," respectively.

The first step in synthesis of the bentonite-alginate MSs was preparation of the aqueous bentonite suspension. The suspension was prepared by dispersion of 0.9 g bentonite powder into 10 cm^3 pure water, followed by its sonification for about 30 min.

Fabrication of the MSs was then effected by mixing of 10 cm^3 of the bentonite suspension with 100 cm^3 of the 3.6% NaALG solution, kneading of the mixture for about 2 hrs by a high speed agitator, and dropwise injection of the obtained sol into 0.1 $mol \cdot dm^{-3}$ $Ca(NO_3)_2$ solution through a 0.3-mm medical needle. As for adjusting of the size of the sol droplets (and thus the prepared MSs) a pneumatic cutting system was utilized that set a controllable air flow around the injection needle (Fig. 1). The formed MSs were gently stirred in the $Ca(NO_3)_2$ solution for about 3 hrs to become hardened, and then they were separated, three folds washed with pure water, and dried at 40°C for about 10 h (19–21). The dried MSs were abbreviated as TK-1.

Some calcium alginate granules (CaALG) were also prepared by injecting pure NaALG sol into $Ca(NO_3)_2$ solution, by following the same pathway as was used for fabrication of TK-1.

Physical Characterization of Bentonite and Microspheres

The particle size, morphology, and the surface structure of both bentonite powder and TK-1 MSs were examined by scanning electron microscopy (SEM, 1455-VP, LEO).

The average composition of the used bentonite was evaluated by X-ray fluoroscopy (XRF, ED2000, ENGLISI OXFORD), and its crystalline structure was revealed through X-ray diffractometry (XRD, STOE STAD-MP) and thermogravimetry analyses (TG, SATA 1500 Scientific Rheometric).

In order to identify the nature of bentonite-alginate bond in the TK-1 MSs, a Fourier transforms spectroscopy (FTIR, Perkin-Elmer PE 2000) was accomplished. The TK-1 MSc for this purpose were first grinded into a

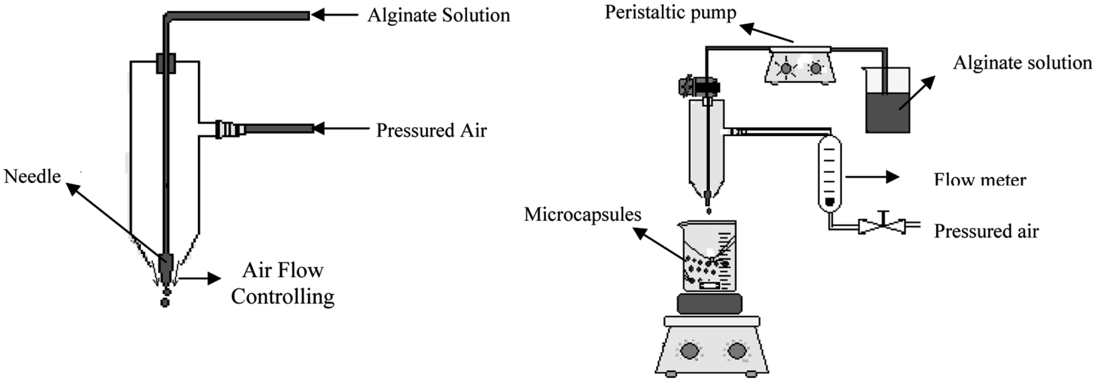

FIG. 1. Schematic illustration of the apparatus used for synthesis of microspheres.

submicron size powder, and then mixed with potassium bromide and pressed into the appropriate plate form of the FTIR analysis. For the sake of comparison, a FTIR analysis of bentonite was also undertaken by following nearly the same procedure as was just mentioned for the MSs.

Porosity of both TK-1 and CaALG MSs was estimated by BET method (QUANT ACHROME NOVA 2200), using nitrogen as the adsorbing gas.

Equilibrium Uptake Experiments

Equilibrium uptake properties of TK-1 MSs, CaALG granules, and bentonite for adsorption of uranyl ion, were studied by using the batch method. An aqueous solution ($10\,cm^3$) of 20–1500 ppm of $UO2^{2+}$ ion was contacted with 0.1 g of the foregoing adsorbents in the propylene test tubes at 25°C, and shaken for about 24 hr. The supernatant then was separated by decanting (in case of TK-1 and CaALG) or filtration (in case of bentonite), and analyzed for uranium by standard Arsenazo III spectrometric method (22,23). Following uptake characteristics were studied using this method:

- Effect of uranium concentration and adsorption isotherm.
- Effect of H^+ concentration from 10^{-4} to $1\,mol \cdot dm^{-3}$.
- Effect of coexisting ions of Mg^{2+}, Ba^{2+}, and Al^{3+} up to 1500 ppm and Na^+ up to $1\,mol \cdot dm^{-3}$.
- Effect of successive adsorption-desorption cycles on the uptake capacity or in other words the reusability of MSs.

Concentration of hydrochloric acid in all experiments (except those devoted to examine the effect of the acid), was $10^{-3}\,mol \cdot dm^{-3}$. Furthermore, $[UO_2^{2+}]$ concentration in majority of the experiments was 200–500 ppm.

In addition to the above experiments, a series of comparative uptake tests were carried out to evaluate the selectivity of CaALG for adsorption of Ag^+ ions in the presence of sodium. In these experiments, nitrate rather than chloride was used as the aqueous counteranion.

Stirred Kinetics Experiments

The apparatus for the study of sorption kinetics was a cylindrical glass vessel with 85 mm inner diameter, whose periphery included three triangular inward projections that acted as baffles. A two-paddle Teflon turbine rotating at 250 RPM agitated the solution. The volume of liquid was $500\,cm^3$ and the mass of adsorbent (TK-1 or CaALG) was 5.1 g.

Column Experiments

An 8-mm-ID glass column packed with 0.25–0.5 g of TK-1 MSs was used for dynamic studies. The flow rate was about $0.4\,cm^3/min$ and concentration of uranium varied from 100 to 300 ppm. After saturating of the MSs column, the bed was eluted by using 6 and $9\,mol \cdot dm^{-3}$ hydrochloric acid solution.

Definitions

In analyses of uptake data, the uptake percentage (R, %), adsorption (Q, mmol/g), distribution coefficient (K_d), and the fraction attainment to equilibrium (X) are defined as:

$$Q = \frac{C_0 - C_e}{m} \times V$$

$$K_d = \frac{C_0 - C_e}{C_e} \times \frac{V}{m}$$

$$X = \frac{C_0 - C_t}{C_0 - C_e}$$

where C_0, C_t, and C_e, are initial concentration, concentration at time t, and at equilibrium (all in $mmol \cdot dm^{-3}$), respectively; V (dm^3) the volume of solutions, and m (g) is the mass of adsorbents.

RESULTS AND DISCUSSION

Characteristics of the Bentonite

Figure 2a exhibits the SEM image of the bentonite powder, and its particle morphology. The average particle size of the bentonite was estimated by standard sieve analysis to be around 40 μm.

The chemical composition of the bentonite, as was obtained from the XRF analysis, is given in Table 1. The amounts of gypsum and other sulfate or phosphate bearing minerals in the sample are negligible. Thus, the calcium and magnesium contents of the bentonite must be essentially bonded to other existing anions such as carbonate and silicate.

The mol percentage of silicate alone in the bentonite is adequately high to electrically balance all available cations, yet the TG analysis of the sample (Fig. 3) revealed two considerable structural changes; first, the weight loss at the temperature less than 200°C corresponds to loss of the physisorbed and interlamellar water. The second weight loss is found in a temperature range 450–700°C. This feature can be interpreted as the expulsion of the structural hydroxyls of the silicate layer (thermal dehydroxylation of silicate structure) which is the beginning of structure change in the bentonite sample.

The XRD pattern of the bentonite (Fig. 4) enlightened its multi-crystalline structure, comprised of the smectite type of montmorillonite as the main constituent, accompanied by quartz, calcite, and albeit as the minor ingredients.

Physical Characteristics of the Microspheres

Figures 2b and 2c exhibit the SEM images of TK-1 MSs along with their surface morphology. The average size of a TK-1 MS is about 300 μm.

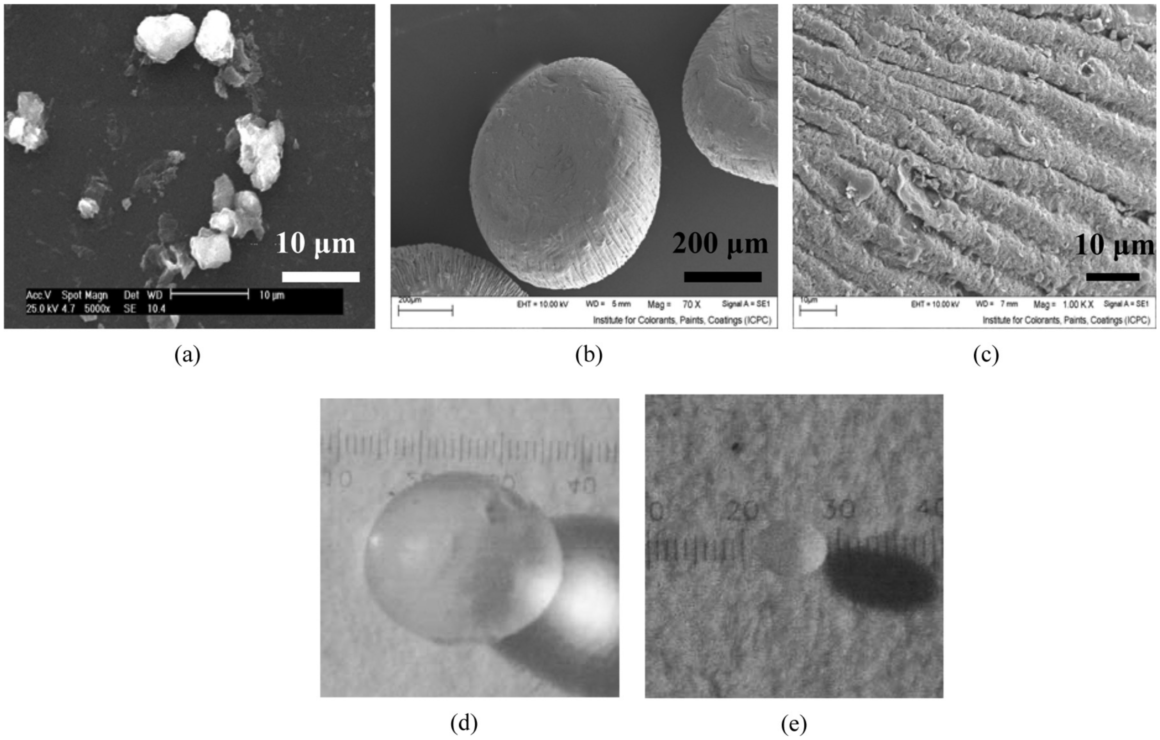

(a) (b) (c)

(d) (e)

FIG. 2. (a) Typical SEM image of bentonite particles, (b) SEM image of TK-1 MCs, (c) SEM surface morphology of TK-1, (d) Optical microscopic image of CaALG before drying, and (e) microscopic image of CaALG after drying.

The specific surface area (SSA) of CaALG that was obtained by BET method ($4.5\,m^2/g$) is in the range of low porosity material. During the drying process, MSs experience volume shrinkage of about 700% (in respect to their final volume). Such immense water evaporation must normally result in a very porous structure; however, the jelly characteristic of the calcium alginate (gel) cancels out this tendency by re-filling of the formed pores and leads to a rather low porosity. Existence of numerous shallow cracks on the surface of TK-1 is a clear sign of its median porosity (Fig. 2c).

In order to further elucidate the abovementioned statement, we prepared two individual samples of the fresh calcium and barium alginate beads and measured their sizes and weights before and after drying. Figures 2d and 2e exhibit shrinkage of the BaALG granules during the drying that corresponds to a volume contraction ratio ($V_{initial}/V_{final}$) of about 28. Interestingly, the corresponding weight ratio was nearly equal to that figure ($W_{initial}/W_{final} \approx 27.5$), implying that the density of both fresh and dried granules were approximately equal. The same results were obtained for the CaALG samples.

Invariable density of the alginate granules during the drying is an evident sign for not creation of the high porosity in the dry BaALG or CaALG samples. In fact, the formation procedure of many of the highly porous materials such as carbon active involves liberation of a great amount of the gas (and thus reduction of the mass), associated with expansion or at least the constancy of the volume. Overall, the density should markedly decrease to give rise to high porosity.

Uptake Equilibrium

Uptake Mechanisms

Both alginate and bentonite constituents of TK-1 MSs have uptake ability for UO_2^{2+} ions, which are of the same extent in different uranium concentrations and pHs (Fig. 5). It is widely adopted that the uptake of uranium

TABLE 1

Chemical composition of the used bentonite as was revealed by XRF analyses

Compound	SiO_2	Al_2O_3	CaO	MgO	SO_3	TiO_2	K_2O	BaO	P_2O_5
Percentage %	75.8	11.9	3.5	1.3	1.6	0.2	0.8	0.5	0.8

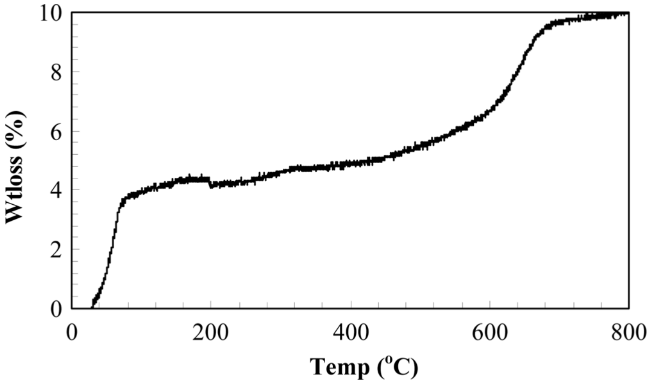

FIG. 3. Thermogravimetric (TG) analysis of bentonite.

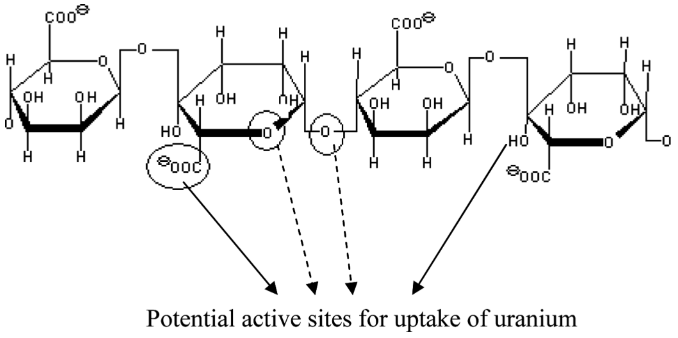

FIG. 5. Molecular structure of alginate, solid and dashed arrows shows the major and minor active sites for $(UO_2)^{2+}$ uptake, respectively.

by alginate proceeds through an ion exchange reaction of following Eq. (1). in which the sequestered uranium in addition to two carboxylic groups, makes the chelation bonds with one or two OH sites of the alginate ring (24), Fig. 5. Overall, uranium forms both trivalent and tetravalent complexes with two adjacent alginate rings. Here, "adjacent" means either two neighbor alginate rings of a single polymeric chain (intramolecular chelation) or two rings from two parallel chains (intermolecular chelation) [see reference 24 for more details]

$$UO_2^{2+} + Ca(ALG)_2 \leftrightarrow UO_2(ALG)_2 + Ca^{2+} \quad (1)$$

For untreated bentonite, as in the case of this current study, the existence of different constituents gives rise to several parallel sorption reactions, yet all of these uptake pathways could be categorized as either surface complexation mechanisms of type Eqs. (2) and (3), or ion exchange reaction denoted by Eq. (4) (8).

$$>SOH + UO_2^{2+} + OH^- \leftrightarrow\ >SOUO_2OH + H^+ \quad (2)$$

$$>SOH + UO_2^{2+} + 3OH^- \leftrightarrow\ >SOUO_2(OH)_3^{2-} + H^+ \quad (3)$$

$$IEY_2\text{-}Ca + UO_2^{2+} \leftrightarrow IEY_2\text{-}UO_2^{2+} + Ca^{2+} \quad (4)$$

In case of bentonite, it has been shown that reaction (4) is more likely to occur in the acidic conditions ($pH < 4$), whereas (2) and (3) are dominant at pH ranges 5–8, and >9, respectively. In addition, the stability constant of the $>SOUO_2OH$ complex is larger than those of reactions (3) and (4), hence the maximum uranium uptake (*R*, %) by bentonite occurs at pHs = 4–8 (8). This is in contrast with the behavior of alginate whose uptake ability is a monotonic ascending function of the pH (19).

Since TK-1 MSs are primarily prepared by the amalgamation of alginate and bentonite, it is expected that their uptake ability (*R*, %) be the arithmetic mean of the uptake ability of their constituents. Surprisingly, this is not the case for the actual behavior of TK-1 MSs. In fact, as Fig. 6 shows, a synergetic effect occurs that makes TK-1 MSs a more effective factor in the uptake of uranium than both of CaALG and bentonite. It is particularly worth noting that TK-1 preserves this superiority in entire ranges of pH and uranium concentration (Fig. 6).

In order to elaborate the aforementioned synergetic effect, we undertook the FTIR analyses of bentonite,

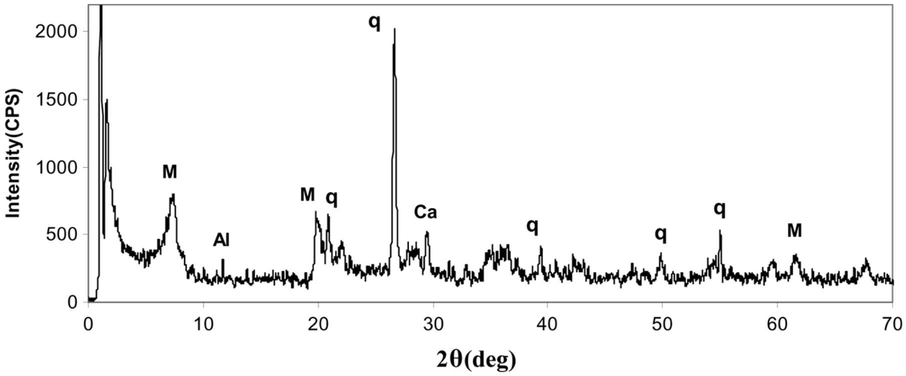

FIG. 4. X-ray diffraction pattern of the employed bentonite; notations correspond to M: montmorillonite, Al: albeit, q: quartz, Ca: calcite.

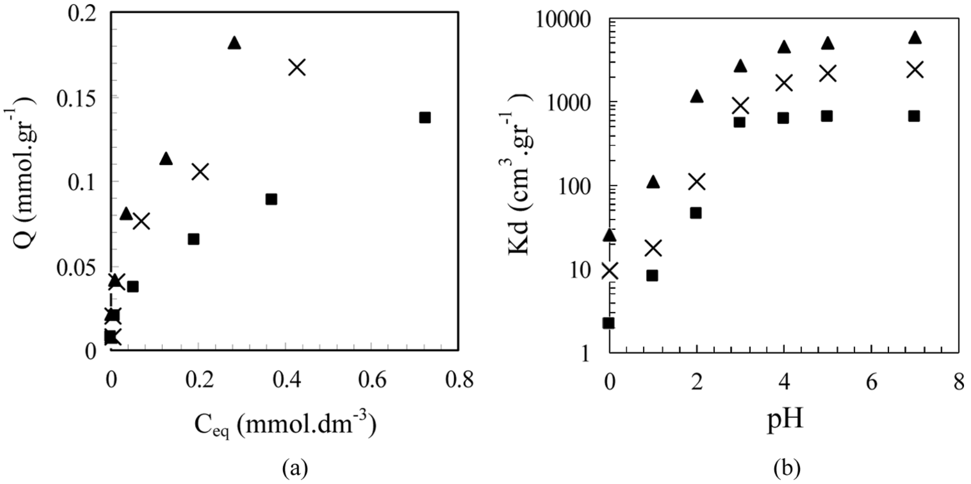

(a) (b)

FIG. 6. (a) Adsorption isotherms and (b) Variation of distribution factor with pH at $[UO_2^{2+}] = 200$ ppm; in both panels; ▲, TK-1; ■, CaALG; ×, bentonite.

calcium alginate, and TK-1 MSs, along with those of alginic acid and sodium alginate for the sake of comparison. The results are shown in Fig. 7.

The IR spectrum of alginate shows absorption bands at around 3450 cm^{-1} (OH stretching), 2900 cm^{-1} (CH stretching), 1610 cm^{-1} (COO$^-$ asymmetric stretching), 1429 cm^{-1} (COO$^-$ symmetric stretching), 1125 cm^{-1} (CO-stretching of ether group), and 1065 cm^{-1} (CO-stretching of alcohol group) (7). The recorded spectra of bentonite include peaks at 3626 cm^{-1} (–OH stretching), 3426 cm^{-1} and 1639 cm^{-1} that respectively are the stretching and bending vibration of the OH group of the adsorbed water, 1383 cm^{-1} is due to CO_3 stretching of calcite, 1034 cm^{-1} assigned to Si-O stretching, and 915 cm^{-1} is due to OH bending of the Al-Al-OH group. A similar OH bending vibration is observed for Al-Mg-OH at 842 cm^{-1}, 796 cm^{-1} is platy form of Tridymite, 690 cm^{-1} assigned to Quartz. Also, there is a shoulder peak at 520 cm^{-1} (Al-O-Si bending), and 466 cm^{-1} (Si-O-Si bending) (12).

Examination of the "TK-1" IR spectrum demonstrates the truth of the above-mentioned speculation that the union of bentonite–alginate is essentially a physical blending (Fig. 7). Almost all peaks of the two raw materials exist in the TK-1 spectrum, with some considerable shifts. This result is not astonishing, because at the time of the preparation of MSs, the major constituents of bentonite (i.e., silicates, carbonates, etc.) react with sodium alginate and then calcium nitrate, merely through some ion exchange (IX) mechanisms. Those IX reactions preserve the molecular framework of the bentonite and alginate, in addition to the identity of the main functional groups.

Although the previous paragraph the reveals the nature of the alginate-bentonite interaction, leaving the main question about the reason for the existing synergetic effect in TK-1 is unanswered. At present, the mechanism of the occurence of this irregular behavior is unknown, and there are just some raw ideas about it as follows:

1. It has been proven that the calcite portion of the untreated bentonite adversely affects its uranium uptake ability probably because a minute release of the carbonate (from calcite) in aqueous media stabilizes uranium in the solution and hinder its adsorption. When bentonite is immobilized in the alginate matrix, possibly a dissolution of carbonate to a lesser extent

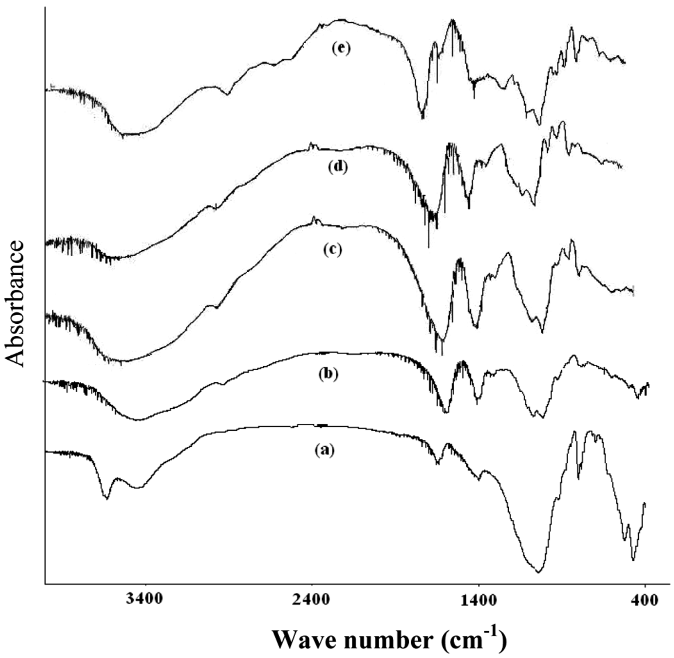

FIG. 7. FTIR spectra of (a) bentonite, (b) TK-1 MCs, (c) calcium alginate, (d) sodium alginate, and (e) alginic acid.

takes place, and uranium complexed with CO_3^{2-} ions is trapped in the MSs (25,26).

2. There is a possibility for the alginate as a carbohydrate to reduce UO_2^{2+} to U^{4+} ions, which may have a greater affinity for sorption on bentonite.
3. According to the previous paragraph, the mixing of bentonite with sodium alginate and then calcium nitrate on the time of synthesis of MSs probably leads to the formation of Ca-bentonite, magnesium alginate, or other similar compounds that probably possess greater uptake ability than the original materials. Since FTIR spectrum of TK-1 does not indicate any considerable chemical alteration, this mechanism is of low importance.
4. In bentonite, as clay normally there is a great portion of nanometric fine particles. Those particles, due to their size effect possess larger surface energy and stronger interaction with water molecules. Therefore, there is a higher possibility for the adsorbed molecules to be stripped from the surface by the large dipole moment of water molecules. Incorporation of the bentonite into alginate matrix reduces the foregoing surface effects, and improves uptake capacity.

Adsorption isotherms of CaALG and TK-1 MSs were fitted with the Freundlich's equation. With the uranium concentration less than 500 ppm, a remarkable fitting was observed from which the following equations were deduced:

$$q_e = 8.04C_e^{0.386} \quad \text{for TK-1} \qquad (5)$$

$$q_e = 3.23C_e^{0.428} \quad \text{for CaALG} \qquad (6)$$

$$q_e = 4.88C_e^{0.448} \quad \text{for Bentonite} \qquad (7)$$

where q (mgU/g) and C_e (ppm) denote the equilibrium adsorption, and concentration, respectively.

Effect of Coexisting Ions TK-1

MSs showed a relatively high selectivity toward uranium over many common coexisting ions (Fig. 8). Of significant importance is the case of sodium, for which MSs maintained their uptake ability even at concentrations as high as $1\,\text{mol}\cdot\text{dm}^{-3}$. When this behavior is compared with the behaviors of pure calcium alginate and pure bentonite (Fig. 8b) in the adsorption of uranium, and that of calcium alginate in the uptake of Ag^+ ions, it immediately follows that:

1. At high Na^+ concentrations, the major adsorbing constituent of MSs is calcium alginate.
2. Coordination rather than ion exchange is involved in the uptake of uranium by alginate.

To further elucidate the latter statement, we had better look more closely at the mechanisms of cations uptake by alginate.

Sequestering of most metal ions by alginate is thought to proceed through the exchange of the target cations (e.g., Ag^+) for calcium ions initially bonded to the carboxylic functional groups (15–18). If this mechanism was held for uptake of uranium also, the adsorption of uranium must have been greatly canceled out by high concentration of competing ions (e.g., Na^+). Uranium is well known for its high tendency for complexation with oxygen atoms of ether, keton, or hydroxyl groups. Indeed, as Hassan et al. (24) have shown, uranium is sequestered by alginate via simultaneous chelation with carboxylic and hydroxyl groups (Fig. 5). Maintaining of the affinity of alginate for

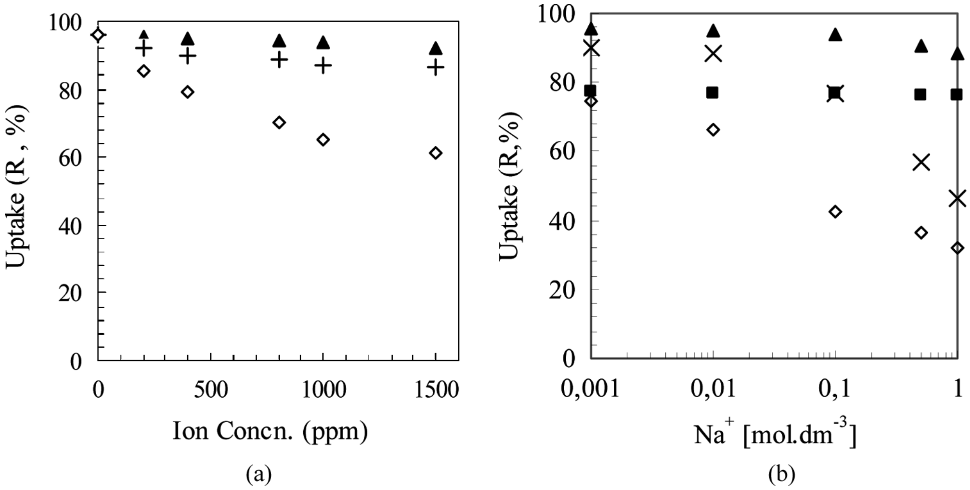

FIG. 8. Selectivity of TK-1 MSs for uranium in presence of different coexisting ions (a) Effects of ▲, Barium; +, Magnesium; ◇, Aluminum; and (b) effect of sodium on adsorption of ▲ $(UO_2)^{2+}$ by TK-1, ■ $(UO_2)^{2+}$ by CaALG, × $(UO_2)^{2+}$ by bentonite, and ◇ Ag^+ by CaALG.

uranium in the presence of Na^+ ions demonstrates that either "UO_2-COOH" bond does not have a simple ionic nature, or alternatively "UO_2-OH" coordination play the major role in chelation of uranium to the alginate.

Still, there is another possibility for uranium to be sequestered by two ethery oxygen atoms in the alginate structure (Fig. 5), but sterical hindrance makes the likelihood of the occurring of this possibility quite unsound.

Uptake Kinetics

Kinetics experiments in the stirred reactor have indicated a relatively fast uptake rate which attains 90% equilibrium level within 30 min (Fig. 9). A fact noting worth which is obtained by plotting the kinetics data in the normalized coordination is that the uptake kinetic of CaALG is always faster than that of TK-1 MSs, while the equilibrium (maximum) uptake percentage has a reversed order.

The phenomenon is similar to what was reported with the adsorption of Ag^+ ions by CaALG and alginate microcapsules enclosing Cyanex 302 extractant (19). Among the different mechanisms standing for these phenomena, apparently the following reasons give a better explanation:

1. The size of calcium alginate granules is smaller than TK-1 MSs, because the drying process of calcium alginate involves a volume reduction of about 2000% (based on its final volume) while a similar figure for TK-1 MSs is about 700%. If the initial size of both adsorbents before drying were similar, the final volume of TK-1 MSs would be about three-fold of CaALG.
2. Referring to the last reason, since the drying process of CaALG is more vigorous, the porosity of the CaALG granule is expected to be greater than TK-1 MSs.
3. A part of TK-1 is consists of bentonite, thus the average (i.e., bulk) diffusion rate of its matrix may be lower than that of CaALG. As it would be seen later in discussion about kinetics models, the rate determining step of kinetics appears to be the slow chemical bonding of uranyl ions to the bentonite or alginate. This chemical reaction retards the diffusion of penetrating ions in TK-1 and explains why its effective diffusion rate must be lower than CaALG.

For modeling of the kinetics, two different approaches were taken, a newer shrinking core model (SCM), and an older pseudo-second order chemical reaction (PSCR).

Advantages of SCM are providing a better physical picture of the uptake process, and the possibility of obtaining diffusion coefficients or the reaction rate constant from kinetics data. There are three different types of shrinking core models which are liquid film resistance SCM, intraparticle resistance SCM, and reaction control SCM. Mathematically, these are represented by the following formulae:

$$X = \frac{3D}{C^0 R\delta}\int_0^t C\,dt \quad \text{Liquid film resistance} \tag{8}$$

$$1 - 3(1-X)^{2/3} + (1-X) = \frac{6D_e}{C^0 R^2}\int_0^t C\,dt \quad \text{Intraparticle resistance} \tag{9}$$

$$1 - (1-X)^{1/3} = \frac{k}{\rho R}\int_0^t C\,dt \quad \text{Reaction-controlled kinetics} \tag{10}$$

where "X" is the fractional attainment to the equilibrium defined by Eq. (3) and C ($mmol/dm^{-3}$) is the concentration

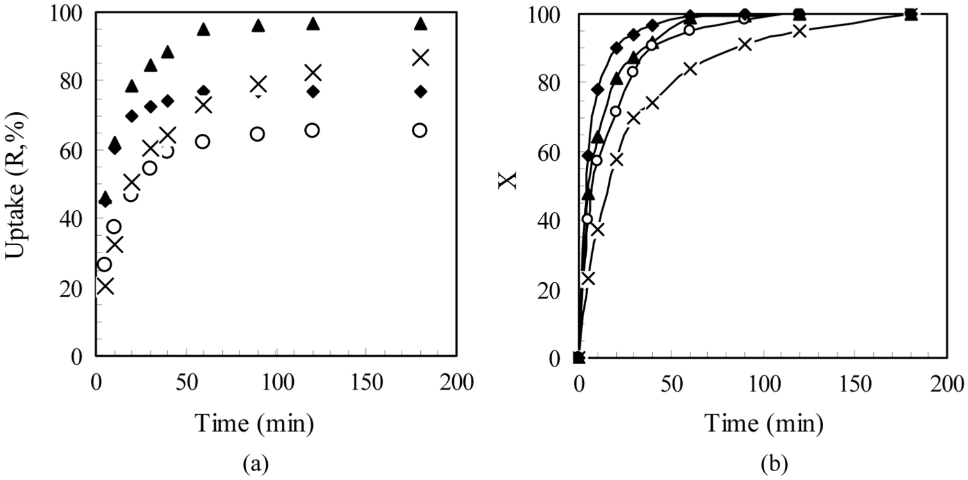

FIG. 9. (a) Kinetics of UO_2^{2+} uptake expressed in term of uptake percentage (R, %) and (b) fractional attainment to the equilibrium (X), In both panels ▲, 200 ppm TK-1; ×, 500 ppm TK-1; ◆, 200 ppm CaALG; ○, 500 ppm CaALG.

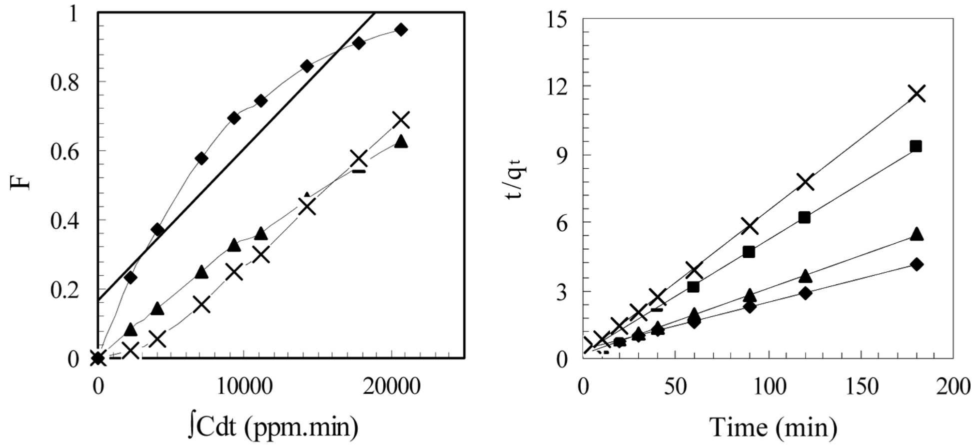

(a) (b)

FIG. 10. Modeling of uptake kinetics by (a) shrinking core model, at 200 ppm [UO_2^{2+}], where ▲, chemical reaction control, × intraparticle resistance, and ◆ liquid film resistance, and (b) by pseudo second order chemical reaction model, where × CaALG, 200 ppm, ■ TK-1, 200 ppm, ▲ CaALG, 500 ppm, and, TK-1, 500 ppm.

at any given time of t, D ($cm^2 \cdot s^{-1}$) and D_e ($cm^2 \cdot s^{-1}$) denote the diffusion rates of liquid film and matrix of MSs, respectively. Also, R (cm) stand for the radius of the particle, and δ (cm) shows the thickness of the liquid film. Other parameters include C^0 the concentration of active sites of the adsorbent ($mmol/dm^{-3}$), ρ (g/cm^3) as its density and finally k'' the rate constant of the adsorption reaction.

The best fitting of the kinetics data was provided by the chemical reaction SCM (Fig. 10), and then by intraparticle resistance SCM. This implies that the rate determining step of the adsorption process is a sluggish chemical reaction of the uranyl ions with the matrix of MSs (i.e., both alginate and bentonite and especially the latter), and to a lesser extent the intraparticle diffusion of the adsorbing ions.

The second kinetics model (i.e., PSCR) assumes that the sorption rate is proportional to the square of the number of unoccupied sites of the adsorbent:

$$\frac{dq}{dt} = k(q_{eq} - q)^2 \tag{11}$$

where q and q_{eq} denote the adsorption values (mmol (uranium)/g (adsorbent)) at time t and in the equilibrium, respectively. The result of application of this model is represented in Fig. 6b. A nearly perfect fitting of the

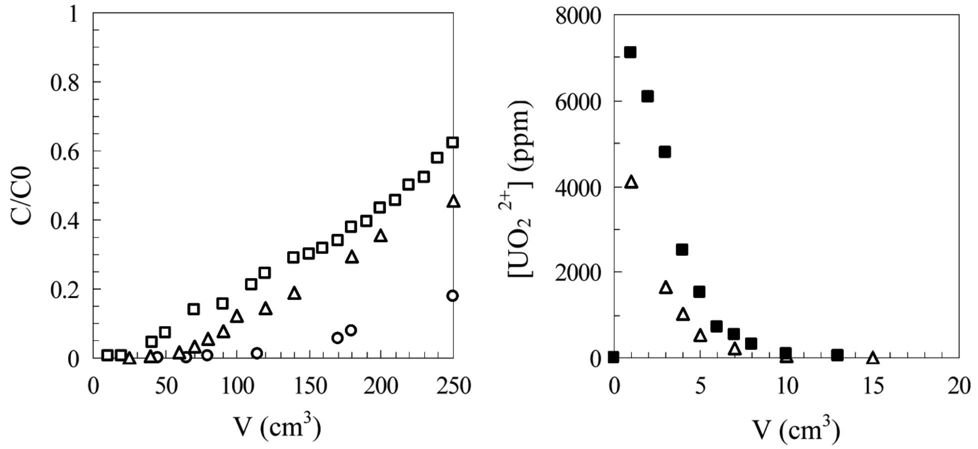

(a) (b)

FIG. 11. (a) Breakthrough curves for UO_2^{2+} adsorption on TK-1 MSs, where: ○ = 100 ppm Δ = 200 ppm, □ = 300 ppm, in all cases flow rate = 0.4 cm^3/min, mass = 0.5 g and [H^+] = 10^{-3} $mol \cdot dm^{-3}$. (b) Elution curves with ■ = HCl 9 $mol \cdot dm^{-3}$ 300 ppm, and Δ = 6 $mol \cdot dm^{-3}$ 200 ppm.

experimental data demonstrates the potential of the model in prediction of the uptake rate and an implicit emphasis on dominating of the chemical reaction in controlling of the sorption kinetics.

Breakthrough and Elution Curves

In the study of column behavior, the effect of concentration, the mass of adsorbent, and the elution behavior were examined. Figure 11a shows the effect of the concentration on the breakthrough curve of TK-1 MSs. In this figure, the breakthrough point that corresponds to the exit condition "$C/C_0 = 0.05$" is approximately inversely proportional to the concentration. Dependency of the breakthrough point to the mass of adsorbent was more complicated and did not follow a linear scheme as did the concentration.

Any adsorbent that is supposed to be employed in the practical separation processes should be desorbed in an inexpensive method, using a commercially available eluent. As an eluent, we used hydrochloric acid with two different concentrations of 6 and $9\,\mathrm{mol \cdot dm^{-3}}$. Figure 11b indicates that both concentrations were effective in fully stripping of the column, but the lower concentration was preferred because of its lesser impact on the TK-1 structure.

Reusability of Microspheres

Another significant characteristic of the commercial adsorbents is their reusability, meaning that the uptake capacity should be maintained in successive adsorption-desorption cycles. In the present study, a batch equilibrium method was used for testing of the reusability by undertaking sorption and elution in shaken test tubes. The results are shown in Fig. 12. It is quite obvious that MSs possess a remarkable reusability.

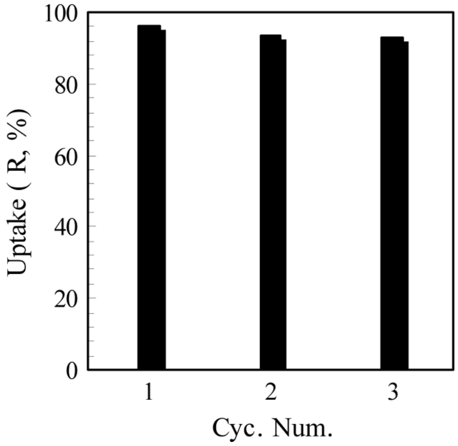

FIG. 12. Reusability of MSs as a function of the adsorption-elution cycle.

CONCLUSIONS

Microencapsulation of bentonite in the calcium alginate matrix presents a simple, but effective method for the synthesis of the selective adsorbents. The prepared microspherical granules are inexpensive, and useful for the removal of toxic heavy metals from aqueous solutions.

Alginate as the immobilizing factor of the active reagents (e.g., bentonite) offers a median level of porosity. This character although is disadvantageous from the standpoint of the sorption kinetics, turned out to be appreciably helpful in the protection of the encapsulated material from leakage.

The TK-1 MSs showed a fairly high selectivity for uranium in the presence of many frequently occurring coexisting ions and at wide range of pHs. The unexpected fact was that TK-1 in spite of being made of bentonite and alginate, presented greater adsorption capacity from both of them. In other words, there was a synergetic uptake effect in the immobilization of the bentonite in alginate. Among the different suggested mechanisms for this phenomenon, the most probable of them, is the elimination of the adverse effect of carbonate (initially exist in the bebntonite) on the uptake of uranium by the immobilization of the bentonite in the alginate matrix.

Another finding of the current study was an evidence for participation of oxygen atom of –OH groups of the alginate in the sorption of uranium. Most of the previous references considered only the involvement of the COOH group in this adsorption.

The uptake of uranyl ions by bentonite-alginate MSs proceed through both surface complexation and ion exchange mechanisms, with the latter prevailing in a wider range of pH, and presenting a greater uptake capacity.

It was shown that uptake kinetics can be modeled by using both the shrinking core model (SCM) and the pseudo-second order chemical reaction model (PSCR). Application of the first model revealed that the rate controlling step of adsorption was primarily a slow chemical reaction of uranyl ions with the active sites of the adsorbing materials especially with those of bentonite. The second (PSCR) model also resulted in a nearly perfect curve fitting, but was less informative in the discovery of the physical picture of the system.

The prepared MSs showed predictable breakthrough properties. In addition, after saturation, they could be easily eluted by using hydrochloric acid. More remarkable is their durability as they can be used in 6 cycles of adsorption-desorption without considerable losses of their capacity.

REFERENCES

1. Olguin, M.T.; Solache-Rios, M.; Acosta, D.; Bosch, P.; Bulbulian, S. (1997) UO_2^{2+} Sorption on bentonite. *J. Radioanal. Nucl. Chem.*, *218* (1): 65.
2. Kublai, S.; Gürkan, R.; Sahan, A.T. (2007) Removal of Cu(II), Zn(II) and Co(II) ions from aqueous solutions by adsorption onto natural bentonite. *Adsorption*, *13* (1): 41.

3. Naseem, R.; Tahir, S.S. (2001) Removal of Pb (II) from aqueous/acid solutions by using bentonite as an adsorbent. *J. Wat. Res.*, *35* (16): 3982.
4. Chakir, A.; Bessiere, J.; Kacemi, K.; Marouf, B.A. (2002) Comparative study of the removal of trivalent chromium from aqueous solutions by bentonite and expanded perlite. *J. Hazard. Mater.*, *95* (1): 29.
5. Dultz, S.; Bors, J. (2000) Organophilic bentonites as adsorbents for Radionuclides II. Chemical and mineralogical properties of HDPy-montmorillonite. *J. Appl. Clay Sci.*, *16* (1): 1.
6. Lazaridis, N.K.; Charalambous, Ch. (2005) Sorptive removal of trivalent and hexavalent chromium from binary aqueous solutions by composite alginate–goethite beads. *J. Wat. Res.*, *39* (18): 4385.
7. Vijaya, Y.; Popuri, S.R.; Boddu, V.M.; Krishnaiah, A. (2008) Modified chitosan and calcium alginate biopolymer sorbents for removal of nickel (II) through adsorption. *J. Carbohydr. Polym.*, *72* (2): 261.
8. Coleman, S.J.; Coronado, P.R.; Maxwell, R.S.; Reynolds, J.G. (2003) Granulated Activated Carbon Modified with Hydrophobic Silica Aerogel-Potential Composite Materials for The Removal of Uranium from Aqueous Solutions. *Environ. Sci. Technol.*, *37* (10): 2286.
9. Dietz, M.L.; Horwitz, E.P.; Sajdak, L.R.; Chiarizia, R. (2001) An improved extraction chromatographic resin for the separation of uranium from acidic nitrate media. *Talanta*, *54* (6): 1173.
10. Kabay, N.; Demircioglu, M.; Yayh, S.; Gunay, E.; Yuksel, M.; Saglam, M.; Streat, M. (1998) Recovery of uranium from phosphoric acid solution using chelating ion-exchange resins. *Ind. Eng. Chem. Res.*, *37* (5): 1983.
11. Davis, T.A.; Volesky, B.; Mucci, A. (2003) A review of the biochemistry of heavy metal biosorption by brown algae. *J. Wat. Res.*, *37* (18): 4311.
12. Missana, T.; Garcý, M.; Alonso, U. (2004) Kinetics and irreversibility of cesium and uranium sorption onto bentonite colloids in a deep granitic environment. *J. Appl. Clay Sci.*, *26* (1): 137.
13. Kaya, A.; Hakan Oren, A. (2005) Adsorption of zinc from aqueous solutions to bentonite. *J. Hazard. Mater.*, *125* (1): 183.
14. Boult, K.A.; Cowper, M.M.; Heath, T.G.; Sato, H.; Shibutani, T.; Yui, M. (1998) Towards an understanding of the sorption of U (VI) and Se (IV) on sodium bentonite. *J. Contamin. Hydrol.*, *35* (1): 141.
15. Ulusoy, U.; Simsek, S.; Ceyhan, O. (2003) Investigations for modification of polyacrylamide-bentonite by phytic acid and its usability in Fe^{+3}, Zn^{+2} and UO_2^{2+} Adsorption. *Adsorption*, *9* (2): 65.
16. Yang, J.; Volseky, B. (1999) Modeling Uranium Proton Ion Exchange in Biosorption. *Environ. Sci. Technol.*, *33* (22): 4079.
17. Gotoh, T.; Matsushima, K.; Kikuchi, K. (2004) Adsorption of Cu and Mn on covalently cross-linked alginate gel beads. *Chemosphere*, *55* (1): 57.
18. De Stefano, C.; Gianguzza, A.; Piazzese, D.; Sammartano, S. (2005) Modeling of proton and metal exchange in the alginate biopolymer. *Anal. Bioanal. Chem.*, *383* (4): 587.
19. Outokesh, M.; Mimura, H.; Niibori, Y.; Tanaka, K. (2006) Equilibrium and kinetics of silver uptake by multinuclear alginate microcapsules comprising an ion exchanger matrix and cyanex 302 organophosphonic Acid Extractant. *Ind. Eng. Chem. Res.*, *45* (10): 3633.
20. Outokesh, M.; Mimura, H.; Niibori, Y.; Tanaka, K. (2006) Preparation of stable alginate microcapsules coated with chitosan or polyethyleneimine for extraction of heavy metal ions. *J. Microencapsulation*, *23* (3): 291.
21. Outokesh, M.; Mimura, H.; Niibori, Y.; Tanaka, K. (2006) Preparation of biopolymeric microcapsules and their uptake properties for the heavy metal ions. *J. Ion Exchange*, *17* (2): 67.
22. Gorecka, H.; Gorecki, H. (1984) Determination of uranium in wet phosphoric acid. *Talanta*, *31* (6): 459.
23. Korkisch, J.; Hubner, H. (1976) Determination of uranium in mineral and rocks. *Talanta*, *23* (4): 283.
24. Hassan, R.M.; Ikeda, Y.; Tomiyasu, H. (1993) Alginate polyelectrolyte ionotropic gels. Part XV Physicochemical properties of uranyl alginate complex especially the chemical equilibrium and electrical conductivity related to the coordination geometry. *J. Mater. Sci.*, *28* (19): 5143.
25. Wazne, M.; Meng, X.; Korfiatis, G.P.; Christodoulatos, C. (2006) Carbonate effects on hexavalent uranium removal from water by nanocrystalline titanium dioxide. *J. Hazard. Mat.*, *136* (1): 47.
26. Dong, W.; Ball, W.P.; Liu, C.; Wang, Z.; Stone, A.T.; Bai, J.; Zachara, J.M. (2005) Influence of calcite and dissolved calcium on uranium (VI) sorption to Hanford subsurface sediment. *Environ. Sci. Technol.*, *39* (20): 7949.